Computer Science Department Technical Report
University of California
Los Angeles, CA 90024-1596

COMPUTER SIMULATION OF BLOOD FLOW IN AN INTRACRANIAL ANEURYSM

M. R. Harreld

April 1993
CSD-930011

TR-930011

Computer Simulation of Blood Flow in an Intracranial Aneurysm

Michael Ray Harreld

April 1993

TR-930011

Computer Simulation of Blood Flow in an Intracranial Aneurysm

Michael Ray Harreld

A Thesis Presented to the
FACULTY OF THE COMPUTER SCIENCE
UNIVERSITY OF CALIFORNIA, LOS ANGELES
In Partial Fulfillment of the Requirements for the Degree
MASTER OF SCIENCE
(Scientific Computing)

April 1993

Acknowledgements

Financial support for this research was provided by the Endovascular Therapy Service, Division of Neuroradiology, Department of Radiological Sciences, UCLA Medical Center.

Special thanks are due Dr. Boris Ayzen and Dr. John Chaloupka. Dr. Ayzen was invaluable for focusing the research, and helping to investigate numerical alternatives. Dr. Chaloupka was instrumental in making this multidisciplinary project successful. Thanks to both for reviewing this paper and recommending improvements.

I thank my advisor, Dr. Walter Karplus, for his guidance and patience at every stage of the project. Thanks also to the other thesis committee members, Dr. Josef Skrzypek and Dr. Jacques Vidal, for reviewing this thesis.

Contents

List Of Figures

Abstract

Intracranial aneurysms are potentially dangerous sacculations arising from an area of weakness within the wall of a cerebral artery. This paper concerns a computer simulation of blood flow in one type of intracranial aneurysm (lateral wall). Geometric data and blood flow parameters were gathered from a surgically constructed in-vivo model of an aneurysm in swine. A computer simulation of three-dimensional steady state Newtonian blood flow through the aneurysm was constructed using the spectral element method. The computer results were visualized and compared to cineangiograms of the animal model. The simulation showed that blood enters the aneurysm at the downstream lip of the aneurysm neck, migrates outward in dual slow helixes around a relatively stagnant core and exits along the lateral edges of the neck. Modeling the aneurysm in three dimensions was found to be crucial for understanding the flow structure.

Glossary

Entries based on Dorland's Medical Dictionary.

Anastamosis Surgical, traumatic, or pathological formation of an opening between two normally distinct spaces or organs.

Aneurysm A sac formed by localized dilatation of an artery or vein.

Angiography Roentgenography of the blood vessels after introduction of a contrast medium.

Atherosclerosis A form of arteriosclerosis in which atheromas containing cholesterol, lipoid material, and lipophages are formed within the intima and inner media of large and medium-sized arteries.

Bolus A concentrated mass of pharmaceutical preparation, e.g., an opaque contrast medium, given intravenously.

Circle of Willis The anastomotic loop of vessels near the base of the brain.

Dilatation The condition, as of an orifice or tubular structure, of being dilated or stretched beyond normal dimensions.

Embolization Therapeutic introduction of a substance into a vessel in order to occlude it.

Fundus The part of a hollow organ farthest from its mouth.

Hematocrit The volume percentage of red blood cells in whole blood.

Hemodynamics The study of the movements of the blood and of the forces concerned therein.

Hemorrhage The escape of blood from the vessels; bleeding.

Ligation A binding.

Lumen The cavity or channel within a tube or tubular organ.

Ostium A mouth or orifice.

Sacculation A pouch, a little bag or sac.

Subarachnoid Between the arachnoid and the pia mater, the innermost membranes covering the brain and spinal cord

Thrombus An aggregation of blood factors, primarily platelets and fibrin with entrapment of cellular elements, frequently causing vascular obstruction at the point of its formation.

Chapter 1

Introduction

Hemodynamics is defined as the study of the movement of the blood and of the forces concerned therein[1]. Analysis of blood flow is important for studying vascular disease. Atherosclerosis and aneurysms are two vascular diseases which have been linked to hemodynamics. Intracranial aneurysms are sacculations arising from a weakened portion of a cerebral artery. These aneurysm are prone to growth and eventual rupture resulting in significant morbidity and mortality. One type of aneurysm is the lateral wall aneurysm which is found on a single parent artery(see Figure 1.1). The focus of this paper is hemodynamics in intracranial lateral wall aneurysms.

With regards to intracranial aneurysms, it is important to gather hemodynamic information for two general uses. In the clinical setting, blood flow structure would be useful data for making prognoses and planning surgery. In aneurysm research, hemodynamic information is important for developing theories of aneurysm growth and rupture.

Intracranial aneurysms are frequently difficult to reach using standard surgical techniques. For this reason, endovascular methods have been developed for treating them. It is now possible to navigate a microcatheter through the arterial system into an aneurysm. Small embolic devices such as platinum coils can then be deposited inside the aneurysm to isolate the aneurysm from the intracranial circulation. This type of surgery has the risk of causing a fatal rupture or stroke.

Angiography is currently the main source of data for therapeutic decision making. Images from angiography provide information on geometry and blood clotting. But hemodynamic data such as velocity, pressure, and shear data are not readily available since it is difficult and risky to directly measure these values. This data would be useful for determining whether a particular aneurysm needed to be operated on, and what course to take during surgery. In general, endovascular aneurysm treatment is dependent not only on geometry and thrombosis (i.e. process of blood clotting), but on hemodynamics[8].

Research is ongoing to determine the cause of aneurysms and to discover the mechanism of their growth. It is known that hemodynamic factors are linked to the etiology of aneurysms, rather than inherited factors[6]. Pathogenesis, growth, thrombosis, and rupture of intracranial aneurysms have been directly related to the effects of hemodynamic forces[17]. In addition to weakness in the vascular wall and hypertension, local hemodynamic features have been found to be partially

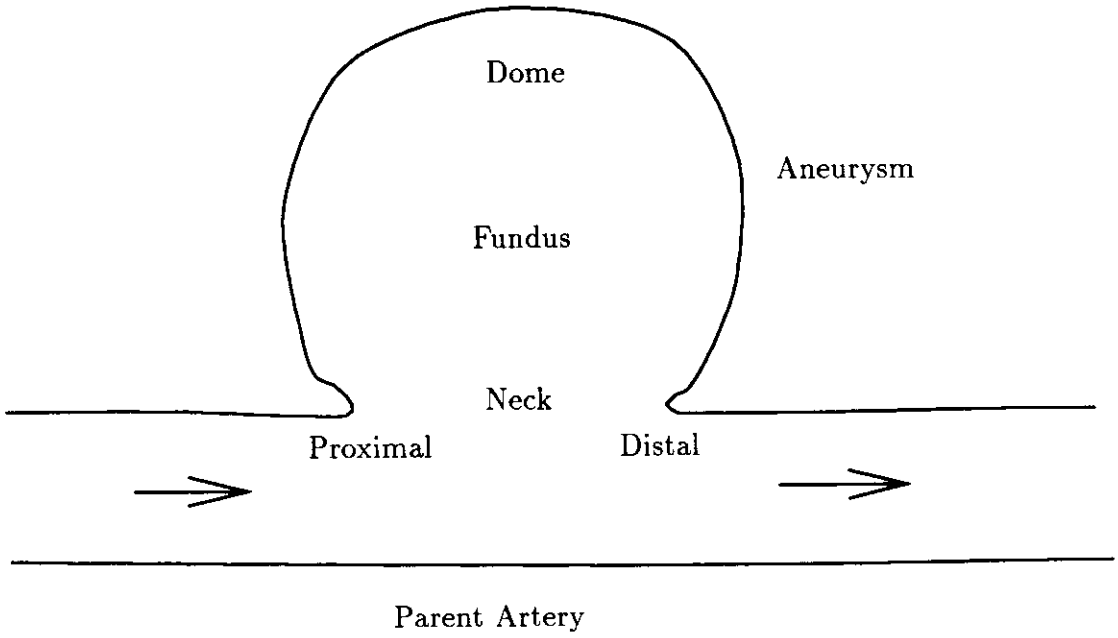

Figure 1.1: Lateral Wall Aneurysm with Terms.

responsible for aneurysm growth and rupture. Clinically this can be shown by the large number of aneurysms found in the arterial loop called the circle of Willis at the base of the brain.[9]

1.1 The Problem

The risk of endovascular surgery for treatment of intracranial aneurysms has decreased, but is still too high to be ignored. One reason that the surgery remains dangerous is that surgeons have limited knowledge of the blood flow structure in aneurysms. This is true for aneurysms in general as well as specific aneurysms encountered in a particular clinical case.

Furthermore, the effect of fluid stress on the behavior of aneurysms is not known. While it is known that the rupture, growth, and thrombosis of aneurysms is linked to hemodynamics, the exact connection has not been found[17].

Since it is currently difficult to reliably predict the risk of rupture of an intracranial aneurysm, some unnecessary endovascular surgeries are inevitably performed. Better understanding of blood flow in aneurysms should help physicians predict whether an aneurysm is likely to rupture, grow, or thrombose[17, 6].

1.1.1 Importance of Research

It is important to investigate aneurysm flow because aneurysms can be debilitating or fatal. It is estimated that the annual rate of rupture of berry aneurysms is roughly 28,000 in North America.

Over half of these ruptures result in death. Intracranial aneurysms are the cause of the majority of nontraumatic subarachnoid hemorrhages and cause 20-25% of all intracranial hemorrhages[13].

1.2 Previous Research

Recent research has been done to investigate blood flow in intracranial aneurysms. Studies have been made based on glass models, cardiometric measurements, and computer simulations of lateral wall aneurysms.

Graves et al.[8] used angiography to study blood flow in dog aneurysms. They found that blood entered the aneurysm in a fast jet in the distal region, traveled in a slow vortex, and then exited more slowly in the proximal region. Blocking or deflecting the inflow or filling the aneurysm with embolic material was found to lead to thrombosis. Position and shape of the embolic material with respect to the inflow zone was determined to be critical to successful embolization.

Strother, Graves, and Rappe[17] further explored blood flow in dog aneurysms with angiography and color doppler methods. It was found that stagnation occurred in the vortex. The inflow zone was comprised of a central fast jet and a surrounding slow region. Disturbed laminar flow was found in the artery just below the neck opening. The flow in aneurysms was found to be not turbulent but predictable, in the laminar and transitional ranges. The hemodynamic stresses were found to vary between different aneurysms.

Liepsch et al.[9] used glass and silastic models with Newtonian and non-Newtonian perfusion fluids to simulate blood flow in aneurysms. It was found that inflow occurred at the distal lip and was directed towards center of the fundus. Outflow was found to occur at the walls of the fundus. They suggested that flow and stress are directly related to pulsatility and viscosity.

Based on in vitro experiments of aneurysms on curved vessels, Niimi, Kawano, and Sugiyama[11] found that curved arteries set up secondary flows which should not be ignored.

Gonzalez et. al.[7] constructed a computer simulation of blood flow in a lateral wall aneurysm. The simulation was based on a two-dimensional model with pulsatile blood flow. Their results showed that there were no inflow or outflow zones into the aneurysm. Blood formed vortices in the aneurysm which reversed direction during the diastolic period. By modeling the aneurysm as two-dimensional, the assumption was made that secondary flow was negligible. This assumption contradicts the findings of Niimi et. al.[11]

It has been suggested that the flow structure in lateral wall aneurysms is inherently three-dimensional. Investigators have reported that flow enters in the distal region and moves in a slow vortex within the aneurysm. Previous researchers have not presented a coherent theory of inflow zone, outflow zone, vortices and stagnation areas.

1.3 Objectives

The main goal of this multidisciplinary research was to demonstrate the feasibility of using a computer simulation to model blood flow in an intracranial aneurysm by comparing in-vivo and numerical results. Other goals were to:

- Analyze the suitability of various simulation methods
- Determine which model simplifications should be refined
- Investigate methods of fluid flow data visualization
- Contribute to the knowledge of blood flow structure in aneurysms

The broader purpose of the research was to begin construction of an aneurysm blood flow simulation system which will have clinical and research applications in the medical field and help increase knowledge of aneurysm etiology, pathology, diagnosis and treatment.

In a clinical setting, results from an aneurysm simulation will be made available to physicians to allow visualization of the flow field in a patient's aneurysm. This will allow identification of critical areas in the aneurysm and help in diagnosis and surgical planning. The simulator will allow plans for endovascular surgery to be tested before an operation begins.

For medical research an aneurysm simulator will allow hemodynamic information to be used in theoretical development. While it is known that there is a link between aneurysm etiology and hemodynamics, there is currently little information about blood flow in aneurysms. The insights gained from viewing blood flow data may provide reinforcement to existing theories or suggest new theories. Furthermore, a computer simulation will be useful for testing new surgical techniques and devices.

1.4 Organization

This paper is divided into seven chapters including introduction and conclusions. Chapter 2 provides an overview of intracranial aneurysms. Chapter 3 presents the specific in-vivo aneurysm model which was simulated. Chapter 4 describes the mathematical model which provided the basis for the aneurysm simulation. Chapter 5 describes the numerical methods used to solve for the hemodynamic characteristics. Chapter 6 covers the implementation of the computer model and the validation of the simulation methods. Appendix A describes *Nekton*, the simulation package used in the project.

Chapter 2

Intracranial Aneurysms

Aneurysms are saccular dilatations of the vascular wall. Intracranial aneurysms are usually located at the base of the brain in the circle of Willis. If they rupture they can cause a catastrophic hemorrhage, often resulting in death. It has been found that 20–25% of all intracranial hemorrhages are caused by intracranial aneurysms[13]. Furthermore, intracranial aneurysms are responsible for the majority of all nontraumatic subarachnoid hemorrhages[13, 6]. This chapter provides an overview of intracranial aneurysms along with a discussion of current theories of their cause.

2.1 Incidence

The true incidence of intracranial aneurysms is uncertain. From general autopsies, the reported occurrence of aneurysms varies from 0.2 to 7.9%. The reported percentage has been found to vary with investigator experience and with the purpose of autopsy. Roughly half of all aneurysms found during autopsy have ruptured[6]

2.2 Classification

Intracranial aneurysms can be classified into several categories. The most commonly occurring type is the saccular aneurysm which comprises 66–90% of all aneurysms. These dilatations are found near an arterial bifurcation in roughly 75% of all cases. Otherwise they are found as lateral wall aneurysms on straight or curved vessels. Saccular aneurysms are often called berry aneurysms because they resemble berries growing on a branch. Unruptured aneurysms are typically found to have diameters from 2 to 10 mm. These smaller aneurysms often have thick necks and thin transparent walls. Aneurysms which have ruptured are usually larger, ranging from 6 to 50 mm in diameter. These aneurysms are sometimes calcified and partially filled with blood clots.[13]

There are other less common varieties of arterial dilatations classified as aneurysms. The fusiform or atherosclerotic aneurysm appears as a region of artery with a local increase in diameter. Mycotic aneurysms are formed by bacteria or fungi which lodge in the artery wall. Dissecting aneurysms occur when the arterial wall is separated forming a pocket which inflates with blood.

2.3 Etiology

There are three competing theories on the cause of intracranial aneurysms. The congenital theory contends that aneurysms are caused by an inherited weakness in the vascular wall. The degeneration theory holds that aneurysms are caused by acquired factors. Hemodynamics and atherosclerosis effects are often cited as mechanisms of the degeneration theory. The third theory is that aneurysms are caused by a combination of inherited and acquired factors.

While the congenital theory has been popular for some time, there is no significant evidence supporting it. There is some evidence for the degenerative theory of aneurysm development which has caused it to be the currently favored theory.[6]

2.4 Symptoms and Diagnosis

It is generally difficult to diagnose an aneurysm before rupture occurs. Sometimes symptoms such as headaches, dizziness, blindness, and neurologic disorders will manifest themselves and prompt testing.

Angiography is the primary means of locating and identifying intracranial aneurysms. The purpose of angiography is to provide the following information about intracranial aneurysms[13]:

1. Identification and location
2. Size and number
3. Neck configuration
4. Evidence of spasm
5. Relation to other arteries

Due to the diffusion of the contrast bolus and the two-dimensional nature of angiograms, it is difficult to determine hemodynamic parameters from angiography. Intravascular methods such as doppler probes allow some measurements to be made of hemodynamic structure. Unfortunately, use of these invasive methods in a clinical setting adds additional risk to either interventional or diagnostic procedures.

There are currently no computer simulation systems which would allow determination of hemodynamic structure in a clinically encountered aneurysm.

Chapter 3

In-Vivo Model

The in-vivo model consisted of a lateral wall aneurysm located on the common carotid artery of a swine. The aneurysm was surgically constructed from a section of vein. The procedure was performed by members of Endovascular Therapy Service and Leo G. Rigler Research Center at the UCLA Medical Center. Angiographic and intravascular physiologic techniques were used to measure geometric and hemodynamic properties of the aneurysm. Several aneurysms were constructed in various swine. The in-vivo aneurysm model used was chosen based on its geometric similarity to typical human intracranial aneurysms.

3.1 Aneurysm Construction

Using standard microsurgical techniques, a side-to-side anastamosis between the common carotid artery and external jugular vein was constructed. A venous pouch was then created by ligation of the external jugular vein around the site of the junction. (see Figure 3.1). Angiography and flow measurements were made several days after the procedure.

3.2 In-Vivo Measurements

Several techniques were used to measure the hemodynamic and geometric properties of the swine aneurysm. Cine digital subtraction angiography (DSA) was performed by bolus injections of iodinated contrast material. This technology provides a thirty frame per second movie of blood flow. Stills from these angiograms were used for determining the geometry of the aneurysm. Figures 3.2 and 3.3 show digitized line drawings of lateral and anteroposterior (AP) angiograms of the swine aneurysm. From the still angiograms, the artery was measured to have a diameter of roughly 3 mm. The aneurysm measures about 14 mm along its largest dimension.

An endovascular Doppler guidewire was used to map velocity in the aneurysm and parent artery at various points. The Doppler device allowed velocity to be measured only along the axis of the probe. A microcatheter connected to a pressure transducer was used to measure pressure at several points within the aneurysm and along the parent artery.

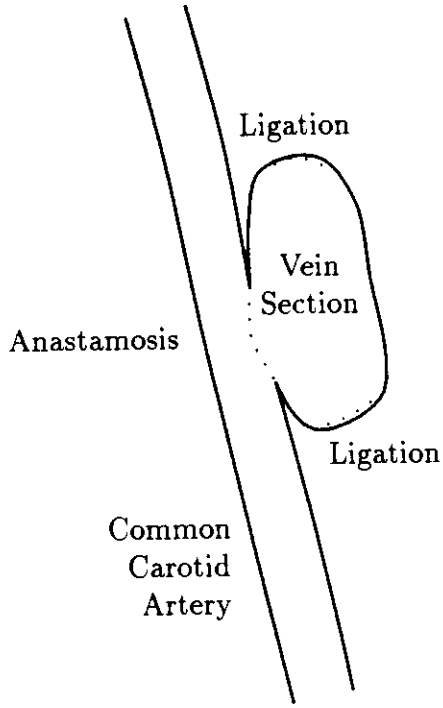

Figure 3.1: Aneurysm Generation by Side To Side Arteriovenous Anastamosis.

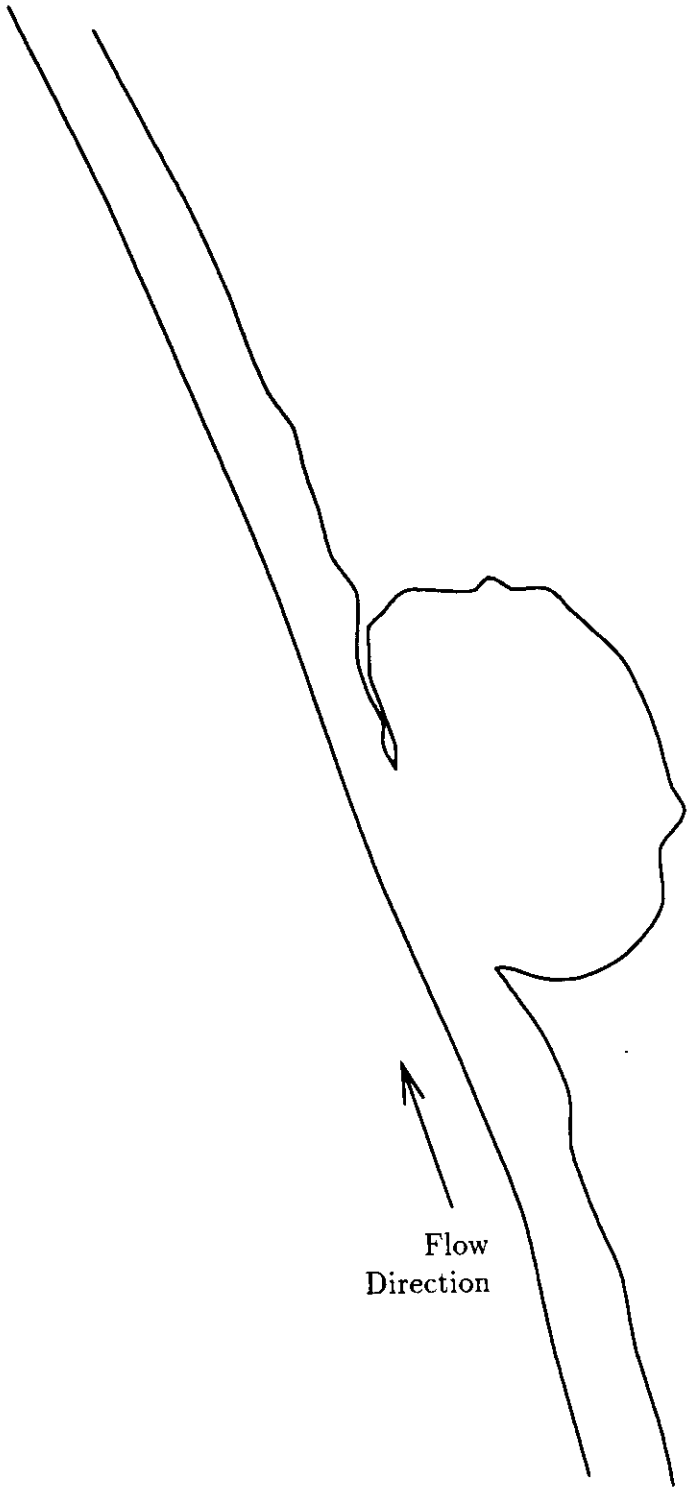

Figure 3.2: Digitized Lateral Angiogram of In-Vivo Aneurysm.

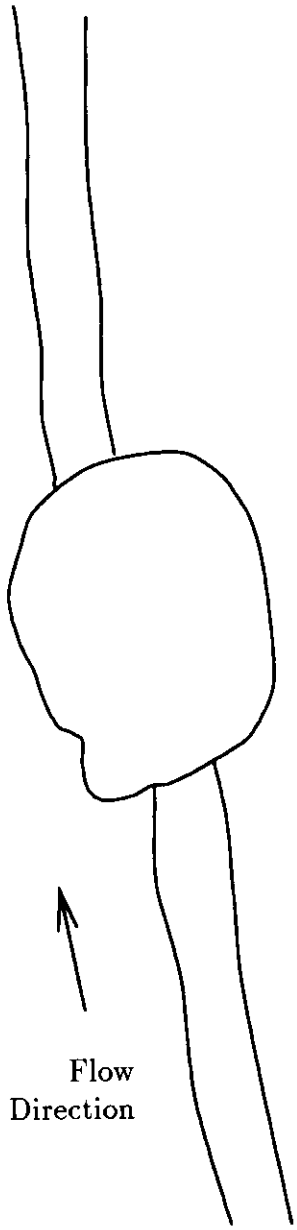

Figure 3.3: Digitized AP Angiogram of In-Vivo Aneurysm.

Chapter 4

Mathematical Model

The mathematical model is described by partial differential equations (PDEs) which govern the general behavior of the flow, and boundary and initial conditions which contribute the specific characteristics of a model.

4.1 Physical System

The physical system modeled was blood flow in a swine artery with an aneurysm. The aneurysm was located lateral to a relatively straight section of the common carotid artery. Blood flow pulsed following the systolic and diastolic portions of the cardiac cycle causing the aneurysm to deform slightly. The blood has non-Newtonian viscosity, and the geometry was not symmetric.

4.2 Simplified Model

In order to build a computer model of the swine aneurysm, several compromises and associated assumptions had to be made. The major simplifications made were:

(1) **Coarse geometry.** The geometry was simplified somewhat for the model. The geometry of the computer model was three-dimensional and slightly asymmetric to match the rough dimensions from the angiograms. Due to the large hexahedral blocks used to build the geometry of the model, the aneurysm wall contours were somewhat coarse. Simplification 1 was considered to be tolerable based on the assumption that sharp corners in the model would collect stagnant fluid and effectively round the walls at those points.

(2) **Artery cross section square.** The swine artery had a roughly circular cross section. The artery was modeled as a square duct. This simplification was made in order to reduce the number of elements so as to decrease computation time. Simplification 2 was based on the assumption that the artery shape away from the neck is not critical.

(3) **Inelastic artery and aneurysm walls.** The walls of the model were considered to be rigid. Though the walls in the swine aneurysm were seen to move slightly, it was impractical to

model the elasticity in the first model. Simplification 3 was justified by the small movements seen in the walls while viewing cineangiograms (angiogram movies) of the swine aneurysm.

(4) Constant blood viscosity. Blood viscosity in the model was considered to be invariant with shear rate, thus the blood was assumed to be Newtonian. Actual blood is known to be non-Newtonian since its viscosity decreases with increasing shear rate. Simplification 4 postulates that the variation of viscosity would only have second order effects on the results.

(5) Constant incoming blood velocity. A constant blood velocity across the inlet section (plug flow) was used in the model. The blood flow was also set constant through time. Both of these conditions are contrary to the pulsatile parabolic velocity profiles in the in-vivo model. The inlet blood speed was set at half of the Doppler measured maximum velocity in the heart cycle. The one half factor was used based on the theoretical constant relating maximum and bulk velocities in parabolic flow. A lead length in the artery was provided to allow the flow to develop to its roughly parabolic profile before reaching the aneurysm. The steady inflow simplification was made to allow a faster non-transient solution to be made. The plug flow boundary condition was made to simplify model construction.

4.2.1 Governing Partial Differential Equations

The fluid is modeled as three-dimensional, incompressible and Newtonian. The flow is governed by the laws of mass and momentum conservation. The Navier-Stokes equation describes momentum conservation in a viscous fluid. It can be written as[3, 5]:

$$\rho(\partial_t \vec{u} + (\vec{u} \cdot \nabla)\vec{u}) = -\nabla p + \mu \nabla^2 \vec{u} \tag{4.1}$$

where ρ is fluid density, $\vec{u}$ is the velocity vector, p is pressure, and μ is viscosity. The ∇ symbol represents the gradient operator and ∂_t represents a partial derivative with respect to time.

The four terms in the Navier-Stokes equation represent balancing contributions to fluid momentum change in an infinitesimal fluid element. The term $\rho \partial_t \vec{u}$ represents the change of momentum with time in a differential element. The term $\rho(\vec{u} \cdot \nabla)\vec{u}$ corresponds to the momentum convected into the element by the flow current. The ∇p term represents change in momentum over time due to net pressure forces acting on an element. The $\mu \nabla^2 \vec{u}$ term corresponds to the momentum change in time from friction induced shear forces.[12] This Newtonian fluid model sets the viscosity μ as constant.

The conservation of mass requirement for incompressible flows can be enforced using the continuity equation[15, 5]:

$$\nabla \cdot \vec{u} = 0 \tag{4.2}$$

Thus the sum of inflows and outflows of an infinitessimal element is zero, and the fluid is incompressible.

In applying these equations to flow in an aneurysm, it must be clearly specified what simplifications are being made. The following are simplifications beyond those in Section 4.2 which come from the statement of the Navier-Stokes and continuity equations:

(6) Incompressible fluid. Simplification 6 is never truly valid, though it is a good assumption for speeds well below the speed of sound.

(7) No heat transfer. Simplification 7 is made since the blood temperature is expected to be relatively constant over the small region of interest surrounding the aneurysm.

(8) No turbulence. Simplification 8 was made based on preliminary calculations of Reynolds number. Reynolds number is a non-dimensional parameter which measures the relative effects of viscous and inertial forces. The Reynolds number (Re) is a nondimensional fluid parameter defined as[3, 15]:

$$Re = \frac{\rho u D}{\mu} \tag{4.3}$$

where ρ is density, u is local speed, D is a characteristic dimension, and μ is the fluid viscosity. It is often used as a predictor of the onset of turbulence. It is expected that when flow in a cylinder has a Reynolds number less than 2000, the flow will remain laminar[15]. Estimates of flow conditions made before simulation allowed an upper bound for Reynolds number in the aneurysm to be calculated at around 600.

4.2.2 Boundary Conditions

The boundary conditions for Equations 4.1 and 4.2 consist of both Dirichlet and Neumann boundary condition types. The Dirichlet or essential boundary conditions are used where only the velocity is specified on a boundary. In this model essential boundaries are the incoming flow and the rigid walls. The Neumann or natural boundary conditions occur where only traction is specified. Natural boundaries in this model occur at the outflow zone.

Boundary conditions were specified along the arterial and aneurysmal surfaces, and along cuts through upstream and downstream sections of the artery. On the walls the velocity was considered to be zero. This essential boundary condition is based on the assumptions that the no slip condition holds and that the walls are rigid. The natural boundary condition at the outflow was specified by assuming that there was a constant zero pressure in the outflow boundary surface. This condition is based on the assumption that the velocity profile has stabilized downstream of the aneurysm. All pressures calculated in the artery and aneurysm are considered to be relative to the outflow pressure.

The inflow boundary condition is more complex than the outflow condition. Ideally, the precise velocity profile across the surface at each point in time should be given. No hemodynamic measurements were available which would determine this velocity profile. The solution to this problem was to move the input boundary farther upstream, and model the input velocity as a simpler profile while still maintaining the proper mass flow rate. The actual input velocity profile

was then modeled as a constant plug flow. As long as the boundary was far enough away from the aneurysm, the deviant velocity profiles due to inexact boundary conditions were resolved before the flow reached the aneurysm.

4.2.3 Initial Conditions

The initial conditions provide a starting point for a transient solution. They consist of a starting velocity field within the system boundaries. Since the system seemed to respond quickly to transients it was convenient and tolerable to start with a zero velocity field.

Initial conditions were prescribed at one instant for each point in the space. Since this simulation was done without pulsatile flow, the initial conditions were not critical. With a pulsatile input velocity, the system becomes cyclic. Initial conditions then become more important. The initial velocities should be the same as the velocities at the end of a cardiac cycle. Thus the initial condition is actually a part of the final solution. The solution to this problem is to guess at an initial internal velocity field and run the simulation through one heartbeat. At this point in time, the flow field should have cycled around to the initial condition. Since the initial condition was guessed at, the final condition will be different and hopefully closer to what would have been the correct initial condition. This refined guess then is fed back into the simulator as a new initial condition. This process continues until the final condition is the same as the initial condition for that particular cycle within some tolerance. At this point the system has achieved periodic steady state and the initial conditions as well as the transient solution have been found.

4.2.4 Constitutive Equation

In a Newtonian fluid, the shear stress is considered to be proportional to its strain rate. The proportionality factor is called the viscosity. For two-dimensional flow, this relationship can be written as[15]:

$$\tau = \mu\dot{\gamma} \tag{4.4}$$

where τ is shear stress, μ is dynamic viscosity, and $\dot{\gamma}$ is strain rate.

Many fluids such as blood or polymeric fluids exhibit non-Newtonian behaviors. These viscoelastic fluids have viscosities which vary depending on factors such as shear rate or shear history. In systems such as this, the viscosity term in Navier-Stokes equations (Equation 4.1) becomes a variable. Therefore an additional relation, called a constitutive equation, is required to solve for the flow field. In non-Newtonian fluids, the constitutive equation describes the nonlinear relation between shear stress and strain rate. For example, the two-dimensional Casson relation is a constitutive equation often used to model blood[10]:

$$\tau^{1/2} = b^{1/2} + s^{1/2}\dot{\gamma}^{1/2} \tag{4.5}$$

where b and s are constants, and $\dot{\gamma}$ is strain rate. In three-dimensional application, $\dot{\gamma}$ is computed based on the second invariant of the shear tensor.

Another possible constitutive equation for blood is the power law model:

$$\tau = A\dot{\gamma}^k \tag{4.6}$$

where A and k are constants. This model for blood viscosity is appropriate in the higher ranges of shear rate.

Chapter 5

Numerical Methods

Once the governing equations with boundary and initial conditions have been prescribed, the problem is ready to be solved. Since an analytical solution is impossible in most complex systems, problems must be converted into a form which can be solved approximately on a digital computer. The specific method chosen for solving the Navier-Stokes and continuity equations was the spectral element method (SEM) which is an extension of the more general method of weighted residuals (MWR). This chapter presents an overview of the method of weighted residuals, a description of the SEM, consideration of other methods, and discussion of commercial software available for computational fluid dynamics (CFD).

5.1 Method of Weighted Residuals

One technique for solving partial differential equations such as the Navier-Stokes equations is to use the method of weighted residuals. The MWR is also known as the Galerkin method[16]. The generalized algorithm corresponding to MWR can be stated in the following form:

1. Construct an approximate solution with unknown parameters
2. Insert this approximation into the differential equation
3. Define the residual to be the difference between approximate and true solution
4. Minimize residual in a weighted sense by:
   - 4.1. Multiplying residual by weighting function
   - 4.2. Integrating the product over the domain of interest
   - 4.3. Setting the result to zero
5. Apply Step 4 using a succession of orthogonal weighting functions
6. Solve for the parameters in the linear algebraic system generated in Step 5
7. Insert the calculated parameters into the approximate solution

The approximate solution constructed in Step 1 is comprised of a set of basis functions (also called shape functions). One method of defining the basis functions is to have them cover the domain in a piecewise continuous fashion. In this way each shape function corresponds to a particular zone in the domain. Another way of defining basis functions is to have each function defined over the entire domain.

The integration in Step 4.2 is performed by first rewriting the integral in the "weak" form. Using integration by parts, the order of the differential equation is lowered by one. This is accomplished by switching differentiation between the weighting function and the dependent variables. The resulting integral can be used to solve for the unknown parameters.[16, 4, 14]

The MWR can be varied by choosing different basis and weighting functions. The method of weighted residuals encompasses the finite element, spectral, and spectral element methods.

5.1.1 Finite Element Method

The finite element method is a commonly used member of the MWR. The method was first used for structural analysis, but has become well established in computational fluid dynamics. In the FEM, the domain is divided into distinct elements. The basis functions are then defined with a one to one correspondence to the elements. Each basis function describes how the solution varies over the respective element. Nodal points are defined as the position in an element where solution will have value of the corresponding parameter. The basis function for one element is defined to be unity at the element nodal point and zero at all other nodal points. The total solution is calculated by summing the products of basis function and corresponding parameters. The basis functions are usually defined as linear or quadratic. The parameters when solved represent the nodal values of the approximate solution over the domain.[4, 14]

The FEM is especially suitable for problems with complex geometries. The method allows an unstructured mesh which can be more easily used to conform to nonorthogonal boundaries. It is simple to refine mesh spacing in critical areas. The FEM is generally quite accurate. There are some weaknesses associated with the finite element method, such as high computation time and memory requirements. The setup work for the FEM is quite universal, i.e. changing a problem parameter will not force a new setup.

5.1.2 Spectral Method

The spectral method is another member in the MWR family. In the spectral method, each basis function is defined globally. Unlike the FEM, each nodal point in the domain has contributions from all basis functions. Common choices for basis functions in the spectral method include Chebyshev and Legendre polynomials. In simple problems the spectral method yields rapid convergence rates. Unfortunately the spectral method has limited usefulness since it is difficult to use with nontrivial geometries.[4]

5.1.3 Spectral Element Method

The spectral element method is an extension to the MWR which combines some of the advantages of the finite element and spectral methods. In this method, the geometry is partitioned into large elements. Since the domain is split into elements, more general complex geometries can be used, as in the FEM. High-order basis functions are defined over each element. This allows rapid convergence of simple fields, as with the spectral method. In this way the SEM overcomes the geometric complexity limitations of the spectral method while taking advantage of its rapid convergence. The spectral element method is advantageous when the solution is relatively smooth and the geometric domain is nontrivial.

Using the SEM, the space domain is divided into hexahedral elements. On each element, a three-dimensional cartesian mesh of collocation points is constructed. Then the dependent variables are expanded over the collocation points as Lagrangian interpolants. These interpolants act as a basis for the solution of the governing equations . The basis is then inserted into the governing equations, and the Galerkin method is used to attain the corresponding algebraic equations. The Galerkin technique is an algorithm for applying the MWR. Convergence of the spatial solution is attained by increasing the number of elements in the domain or the number of collocation points per element.[4]

Based on the assumption that flow within the aneurysm would be smooth, the SEM was chosen for solving the Navier-Stokes and continuity equations in the aneurysm model.

5.2 Comparison of SEM and FEM

The spectral element and finite element methods belong to the general family of weighted residual methods. The FEM uses a piecewise linear or quadratic function for forming a basis over many discrete elements. The SEM uses a more complex basis consisting of higher order polynomials defined over typically larger elements. The solution to a SEM is then a smooth interpolation of collocation points. Figure 5.1 illustrates the difference in solution between the two methods.

The advantage of the SEM is that it provides fast convergence when solving smooth fields. The speed is due to the assumption of smoothness inherent in the method. The disadvantage of the SEM is that a field with high gradients will force small elements to be used which will compromise the speed gains. The FEM with its typically finer meshes is more suitable for fields with high gradients. Large changes can occur across grid points without disrupting adjacent calculations.

For low Reynolds number problems, the spectral element method takes advantage of the smooth transitions in the flow to yield faster convergence times than the FEM. Since the grid elements are larger, manual grid construction is faster, but constructing fine detailed meshes is more difficult.

5.3 Temporal Solution

In order to decrease solution time, the method of characteristics was used to solve the time dependent Navier-Stokes equation. Using this method convective and diffusion terms of the Navier-Stokes

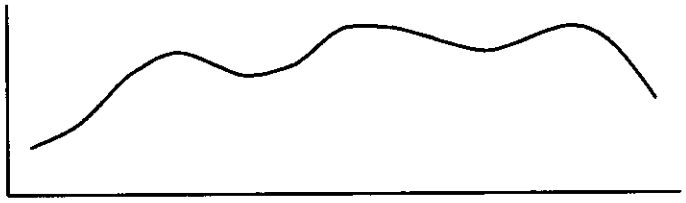

True Solution

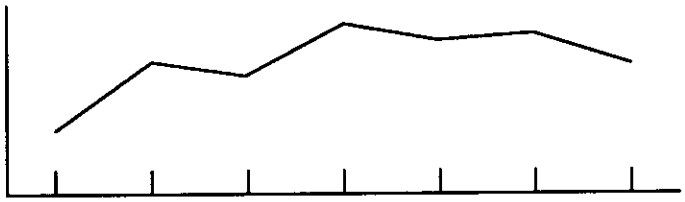

Finite Element Method Solution
6 Linear Elements

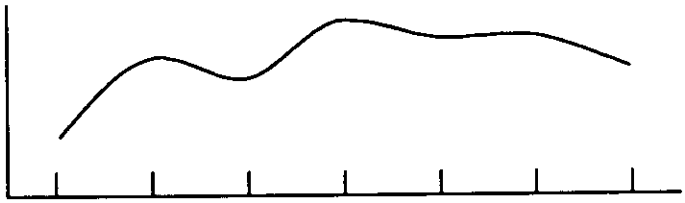

Spectral Element Method Solution
One 7th Order Element

Figure 5.1: Illustration of FEM and SEM Solutions.

equation were solved using different time steps. The convective term, $\rho(\vec{u} \cdot \nabla)\vec{u}$, was treated explicitly. A third-order Adams-Bashforth multistep method was used yielding temporal accuracy of Δt^3, where Δt is the time step size. An explicit method was used for the convective term to avoid solving a nonlinear set of algebraic equations at every time step. The tradeoff was that requirements on Δt must be made to ensure stability.

Using the method of characteristics, the diffusion terms $\mu\nabla^2\vec{u}$ and $\nabla \cdot \vec{u}$ were treated implicitly. A second-order backward differentiation multistep scheme was used with accuracy on the order of Δt^2. This computation was automatically stable, but a set of linear algebraic equations had to be solved at each time step. An iterative solver was used to compute results to these equations.[5]

5.4 Preparation for Solution

In order to solve a fluid system using the SEM, the problem had to be defined in a specific way. A geometric grid of hexahedral elements was constructed. The density and viscosity of the fluid had to be defined. Initial conditions were specified for each point in the space. Boundary conditions were specified on the outer faces of the elements for each instant of time. The order of the spectral elements was declared. Finally, a solution strategy had to be chosen.

5.5 Alternate Methods

Besides the FEM and spectral method, two other methods were considered as alternatives to the spectral element method. The SEM was chosen because it was expected to yield fast convergence with high accuracy for laminar flows. The other two methods which were considered were the finite volume method and the boundary element method.

5.5.1 Finite Volume Method

The finite volume method (FVM) discretizes a fluid field as an orthogonal grid (e.g. cartesian or polar). A set of algebraic equations is generated by approximating the partial differential equations with appropriate finite difference equations local to each node. The FVM is also known as the finite difference method, the method of collocation, and the subdomain method. At its root, the FVM is another variation of the MWR, though its implementation is simpler than most of the other methods. The finite volume method has a successful history of use on computational fluid dynamic (CFD) problems.[12, 4]

Coding FVM systems is easier than the other methods, and the programs tend to have acceptable performance. One significant drawback is the orthonormal grid imposed by the method. This requirement makes complex geometries difficult to represent. Some commercial FVM packages have sought to overcome this limitation by introducing body fitted coordinate systems. Accuracy of the FVM is typically lower than the other more complex methods. Finite volume methods are often used for high Reynolds number problems.

5.5.2 Boundary Element Method

The boundary element method (BEM) is based on Green's Theorem. The method involves integrating to find the interior of an element based on the function along its surface. It is difficult to simply introduce new effects into a problem since this fundamentally alters the mathematics. The method only yields a solution on the element boundaries, and does not supply interior values. The BEM has only recently been used for CFD. It is a highly mathematical method and requires significant initial preparation.

Problems best suited to the BEM are those with high gradients and infinite boundaries. Most applications are in turbulent and sonic flow. The method yields good convergence rates, but is difficult to implement due to the mathematical expertise required during programming.[2]

5.6 Computational Fluid Dynamics Software

There are a variety of commercial CFD packages available. They vary in types of flows simulated (e.g. laminar, transient, compressible), numerical methods used, and user interfaces (text or graphics based). Several commercial CFD packages were considered for aneurysm blood flow simulation. They consisted of software packages implementing the finite element method, the finite volume method, and the spectral element method. The packages were compared based on the following criteria:

- Ease of grid generation
- User interface
- Relative performance
- Accuracy
- Availability and support
- Visualization capabilities

Considered CFD packages included:

EasyFlow FVM package for general flow[1]

Fidap FEM package for general flow[2]

Flow3D FVM package with unstructured mesh[3]

Fluent FVM package with body fitting mesh for general flow[4]

[1] Flowsolve
[2] Fluid Dynamics International
[3] Computational Fluid Dynamics Services
[4] Fluent Incorporated

Nekton SEM package for laminar flow[5]

P/Flotran FEM package for general flow[6]

Phoenics FVM package for general flow[7]

Rampant FEM package for compressible flows[8]

The most promising package from each method was selected. The three packages, *Fidap* (FEM), *Phoenics* (FVM) and *Nekton* (SEM), were then compared against each other. The FVM package was removed from consideration for reasons of accuracy and grid generation constraints. The SEM code *Nekton* (see Appendix A) was finally chosen based on the assumption that the gradients in the aneurysm blood flow would be low.

After simulating the blood flow, it was found that velocity gradients were low along the direction of the streamlines. The gradients across the streamlines (shear rate) were quite high in areas around the inflow jet and aneurysm vortices. The choice of SEM software was thus based on an invalid assumption. It would be useful to compare performance and accuracy between the FEM and the SEM to better judge the consequences of high shear rate.

[5] Fluent Incorporated
[6] PDA Engineering
[7] Concentration Heat and Momentum Limited
[8] Fluent Incorporated

Chapter 6

Validation

This chapter presents an implementation of the aneurysm model presented in Chapter 4 using the numerical techniques of Chapter 5. A computer simulation of the swine aneurysm described in Chapter 3 is described along with data from both the experimental and computer models.

6.1 Computer Model

The computer simulation of the swine aneurysm was built using the general purpose spectral element method (SEM) computational fluid dynamics (CFD) package *Nekton*. Fluid parameters were taken from estimated blood characteristics. The aneurysm geometry was based on angiograms taken of the swine aneurysm. The simulation was run on a Sun Sparcstation.

6.1.1 Model Prototyping

Before building the aneurysm model highlighted in this paper, a series of incremental models was constructed. The first model was two-dimensional: a circular aneurysm on a straight artery. After several remeshings, a converged solution emerged. The results agreed with those of Gonzalez et. al. [7]. No distal flow entry or proximal exit were found at the aneurysm neck. Since this was contrary to angiographic evidence, the model was expanded to be three-dimensional.

The second phase was to implement a very simple three-dimensional aneurysm model. The aneurysm was modeled as a box adjoined to a square duct. This model was refined until the solution converged. Studying this simple three-dimensional model gave some insight into what the complexity of the more advanced models would be. The prototypes also allowed different numerical methods and assumptions to be tested for effects on accuracy and convergence time.

The third phase of modeling was to experiment with different meshing schemes. The goal was to find a grid style which would allow large elements in areas of expected low flow gradient and small elements in areas with expected high gradients. Particular attention was paid to finding a scheme which allowed high geometric detail in the neck. Once an optimal meshing strategy was found, a similar mesh representing the geometry of the experimental aneurysm was constructed based on angiographic images.

6.1.2 Modeling Procedure

The general procedure for building a working model involved iteration. First a fundamental grid which most simply modeled the angiographic images of the aneurysm was built. This mesh was used for a fifth order simulation run. The velocity and pressure results were examined qualitatively for discontinuities across element interfaces, and wiggles within elements. The divergence field was examined for maxima and minima. The areas which showed discontinuities, wiggles and extreme divergence were singled out for refinement. The mesh was divided into smaller elements in these problem areas. In this way the density of the mesh elements was made to match the areas of high gradients. The new mesh was then resubmitted for solution, and the process continued. When the trouble areas had been eliminated the order of the solution polynomials was raised from five to seven and the solution was recomputed with the same grid. Since this had a minor affect on the solution, it was assumed that the solution was order independent and had converged.

6.1.3 Geometry

The source for the computer model geometry was lateral and anteroposterior (AP) angiogram images of the swine aneurysm and artery(see Figures 3.2 and 3.3). A three dimensional mesh of spectral elements was constructed based on the dimensions and shape of the aneurysm. During the preliminary phases of modeling it was found that aneurysm neck size and shape had a strong effect on the flow pattern. For example, making the neck long and narrow lead to proximal entry, while short wide necks yielded distal flow entry. Therefore special attention was placed on accurately modeling this region of the mesh.

To reduce the number of elements, the artery was modeled as a square duct. This was considered tolerable since the flow in the corners was fairly stagnant and thus the velocity in the computer model artery took on a relatively cylindrical profile. The total number of spectral elements was 61. The mesh is shown in Figure 6.1. Each hexahedral spectral element had 125 collocation points defined within it.

6.1.4 Flow Parameters

The density of the blood was modeled as 1240 kg/m^3. This is a typical value found in the literature. The dynamic viscosity was considered as a constant 0.03 $N \cdot s/m^2$. Since blood is non-Newtonian, the viscosity varies with shear rate. The actual viscosities measured in blood vary over several orders of magnitude. [18] The value for viscosity was picked from the middle of the range.

6.2 Results

Results are presented here for one of the experimental swine aneurysms (see Chapter 3 for description of construction), and the corresponding computer model.

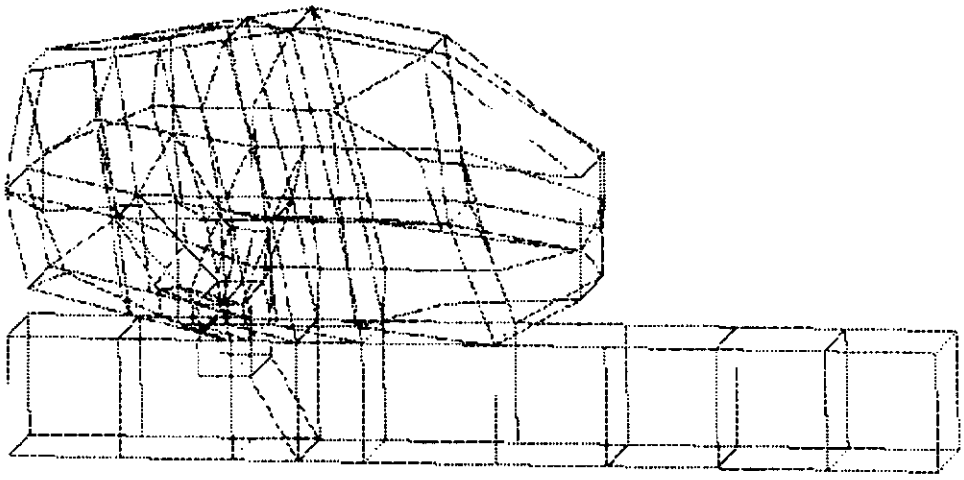

Figure 6.1: View of Aneurysm Model Spectral Element Mesh.

6.2.1 Experimental Results

The hemodynamic results for the experimental swine aneurysm came from 30 frame/sec cineangiograms, doppler velocity probe measurements, and endovascular pressure transducer readings.

The cineangiograms were taken in lateral and AP views. The videos showed blood entry at the distal lip of the ostium. An inflow jet could be seen curling up along the fundus. The contrast slowed rapidly after it entered the aneurysm. A slow vortex could be seen in the lateral plane. A central core of fluid could be seen to be isolated from the main flow. Contrast material slowly diffused into this core. No outflow zone could be identified.

Using the doppler probe, velocities were measured in different areas of the aneurysm and parent artery. Traces from the doppler probe showed a prominent distal jet, and low velocities within the aneurysm. The jet had speeds in the vicinity of 30% of arterial flow. Speeds in the aneurysm away from the inflow jet were in the 5% to 15% range.

Measurements made with the endovascular pressure transducer showed the pressure within the aneurysm around the fundus and along the artery. The pressure within the aneurysm was relatively constant with the same value as the artery at the neck. Following the direction of blood flow, the centerline pressure was found to drop smoothly until the aneurysm neck. At this point it spiked up at the proximal lip, dove down along the ostium, rose up at the distal lip, and then resumed a gradual drop along the artery(see Figure 6.2). The mean pressure loss rate in the artery was calculated as 31 kPa/m. The sketch above the graph indicates where the measurements were taken. Mean pressure within the aneurysm was found to vary between 125 and 128 $mmHg$.

6.2.2 Computer Results

The computer results consisted of velocity and pressure values at the collocation points within the model. These data were visualized using both the Nekton postprocessor and the fluid visualization

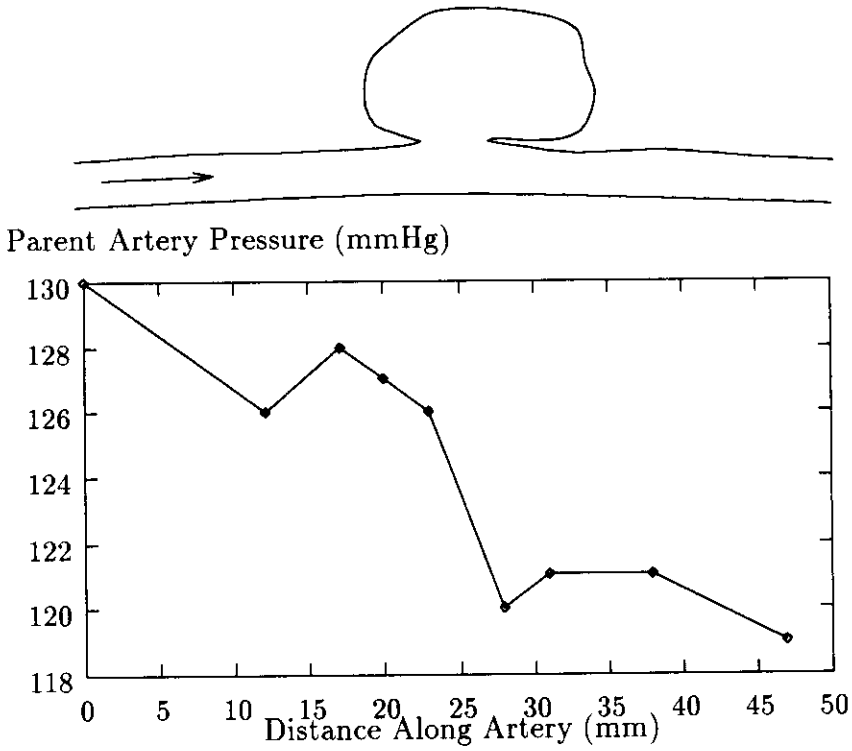

Figure 6.2: Mean Pressure Along Swine Artery.

package Data Visualizer(Wavefront Technologies). In addition to velocity and pressure, integrated streamlines were viewed with the visualization software.

The pressure within the simulated aneurysm was found to be virtually constant. Following the flow direction, the pressure gradually decreased until the proximal region of the ostium. Along the neck the pressure was relatively constant at the same value as within the lumen of the aneurysm. After the distal lip, the pressure resumed its gradual drop. The mean pressure loss rate in the artery was calculated as 64 kPa/m.

A complex flow pattern was found in the computer aneurysm which can be characterized by the following features:

- Fast arterial flow hump rises in ostium
- Inflow jet located centrally in distal ostium
- Flow in aneurysm moves in slow helical pattern
- Axis of helix curves laterally downward
- Outflow occurs at lateral edge of ostium
- Helixes travel around slow moving lumen core

The inflow zone, outflow zone, and shape of the streamline helix are shown by Figures 6.3 and 6.4. The flow hump, inflow jet, and slow core can be seen in Figure 6.5. Figure 6.5 shows the speed drop from 20%+(black) to 0%(white) of the maximum arterial flow along a central cutting plane..

6.3 Comparison of Experimental and Computer Results

To validate the computer model, qualitative and quantitative comparisons were made between the experimental and computer results.

Qualitatively, the experimental and computer model results shared many characteristics. Both had a prominent distal inflow jet. Both had an internal slow moving separated core. Both showed secondary flow, i.e. flow components in the lateral direction.

Numeric results which could be compared consisted of pressure drop along the artery, and jet inflow speed. The pressure drop rate in the experimental model was roughly half that in the computer model. This suggests that the viscosity in the computer model should be decreased. The actual pressure drop profiles differed somewhat between the computer and experimental models. The computer model showed a flat pressure profile along the aneurysm neck, with a smooth transition. The experimental model showed a high pressure spike at the proximal lip, a steep pressure drop across the neck, and a low pressure spike at the distal lip. The source of this phenomena is unknown. Both models held a virtually constant pressure within the aneurysm.

The relative jet speed just inside the aneurysm in the experimental model was roughly twice that computed in the simulation. This could be due to difference in the neck configuration between the models.

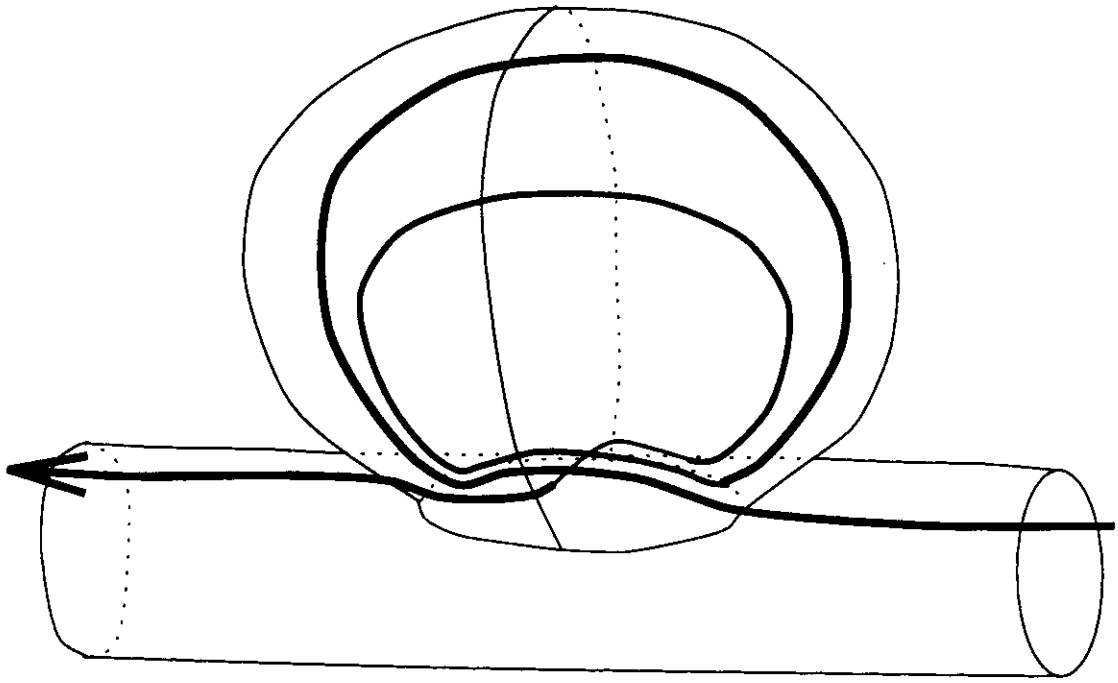

Figure 6.3: Drawing of Isometric View of Helical Flow in Aneurysm.

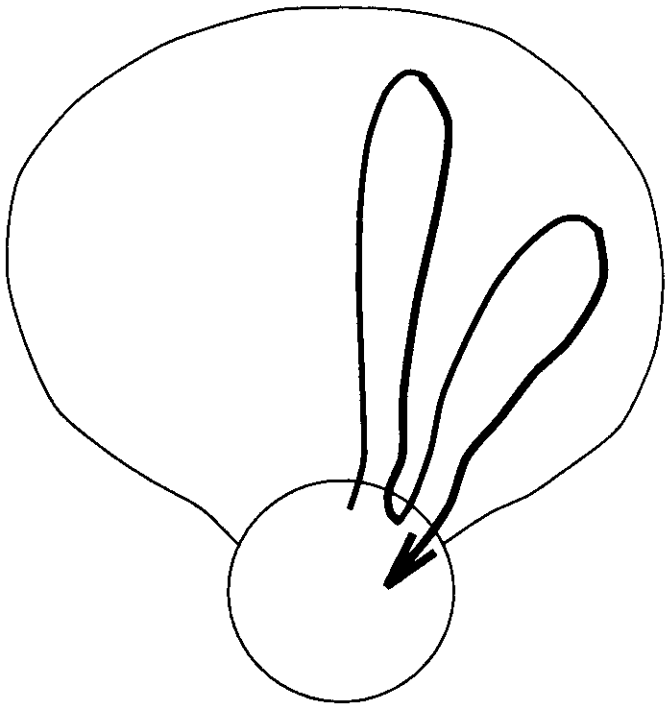

Figure 6.4: Drawing of Axial View of Helical Flow in Aneurysm.

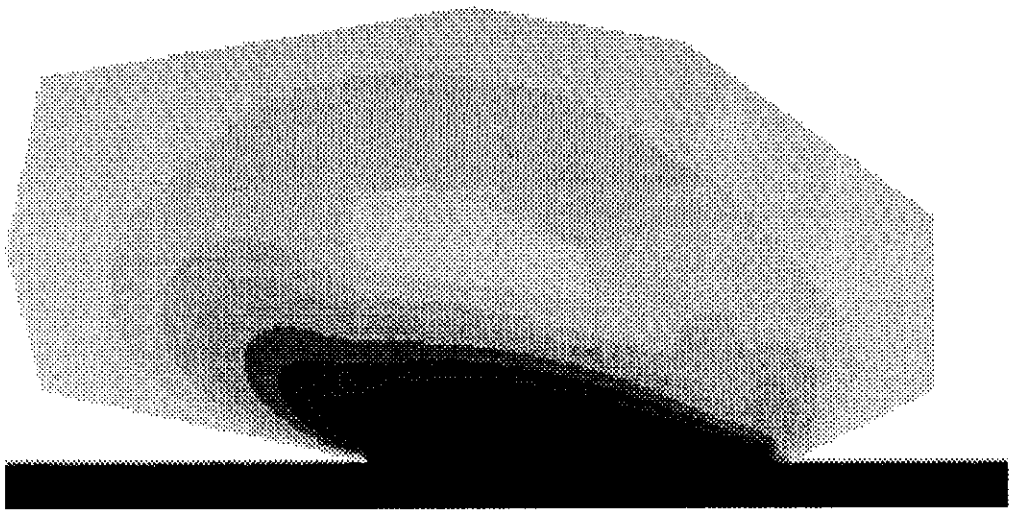

Figure 6.5: Lateral View of Speed in Computer Aneurysm.

Chapter 7

Conclusions

It is feasible to computer simulate blood flow in intracranial aneurysms. With a quite simple model, we were able to simulate an experimentally generated aneurysm and compare results. This first model allowed development of a comprehensive new theory for blood flow structure in lateral wall aneurysms.

7.1 Comparison with Previous Research

The results of this simulation indicate that secondary flow is crucial and that a three dimensional model is necessary to accurately model aneurysm flow. This finding disagrees with the results of Gonzalez et al.[7] who found that there was flow reversal rather than inflow in their two-dimensional model, and assumed that secondary flow was negligible.

7.2 Advantages of Three Dimensional Model

The flow structure computed with the computer simulation showed prominent secondary flow. This lateral velocity component was necessary to allow central distal inflow to move to a side outflow zone. With a two dimensional model, this type of flow is impossible. Either flow enters in the proximal region, or it is forced into reversal[7] with no inflow zone. Neither of these two patterns was seen in the angiographic studies supporting this research.

7.3 Spectral Element Method in Computational Hemodynamics

The decision to use the SEM was based on the assumption that the flow gradients would be low within the system. After completing the first generation aneurysm simulation, it seems this may have been an inaccurate assumption. High gradients occur in the aneurysm between the inflow jet and surrounding fluid and in the ostium between the fast hump and the slow core. Another problem encountered with the SEM was that using large elements discouraged making smooth

natural meshes. For these two reasons, it would be worthwhile to try a finite element method system for purposes of comparing performance, accuracy, and mesh generation.

7.4 Further Research

The next step in this research will be to add two features to the aneurysm model: pulsatile flow and non-Newtonian blood. The pulsatile flow will be a incoming velocity variation with time. The relation of velocity and time will come from doppler velocity strip charts taken within the swine parent artery. The non-Newtonian blood model will allow blood viscosity to vary with shear rate. This relation will be based on data in the literature and may be modeled with a power law or using the Casson relation.

New experimental models will be simulated using more refined meshes. Validity of the computer model will be investigated more thoroughly using the culminated experience of the multidisciplinary team. Bifurcation and terminal aneurysms make up the majority of naturally occurring intracranial aneurysms, and should be included in the simulation effort. These aneurysms will bring new challenges to modeling, visualizing and validating.

One promising research direction is to investigate the effects of elasticity in the aneurysm wall. The combination of stress within the wall, internal hemodynamic forces and external tissue resistance act to move the aneurysm. Over a short time period, this movement occurs as the aneurysm throbs in response to the heart beat. This periodic flexing could contribute to weakness and eventual rupture. Over an extended time, these forces may act to cause the gradual growth of an aneurysm.

Beyond model improvement, new methods of visualization will be investigated. Analyzing transient three-dimensional flow data is very cumbersome using a flat screen and simple software. A more complex immersive interactive environment (Virtual Reality) would be well suited to the task of aneurysm flow visualization.

7.5 Contributions of the Research

We have shown that it is feasible to make a computer simulation of an aneurysm which is verifiable against in vivo models. A theory of blood flow structure in lateral wall aneurysms has been presented which links together the previous observations of distal inflow, stagnant core, and secondary flow. This coherent theory relates inflow zone, outflow zone, vortices and stagnation areas. The results imply that two-dimensional aneurysm models are inadequate.

Reference List

[1] Douglas M. Anderson, editor. *Dorland's Pocket Medical Dictionary.* W. B. Saunders Co., 24th edition, 1989.

[2] P. K. Banerjee and L. Morino, editors. *Boundary Element Methods in Nonlinear Fluid Dynamics.* Elsevier Applied Science, 1990.

[3] Robert S. Brodkey. *The Phenomena Of Fluid Motions.* Addison-Wesley Publishing Company, 1967.

[4] Fluent Inc., Centerra Resource Park, 10 Cavendish Court, Lebanon, NH 03766. *NEKTON Version 2.85 Theory.*

[5] Fluent Inc., Centerra Resource Park, 10 Cavendish Court, Lebanon, NH 03766. *NEKTON Version 2.85 User's Guide.*

[6] John L. Fox. *Intracranial Aneurysms*, volume 1. Springer-Verlag, 1983.

[7] Carlos F. Gonzalez, Young I. Cho, Hector V. Ortega, and Jacgues Moret. Intracranial aneurysms: Flow analysis of their origin and progression. *AJNR*, 13:181–188, February 1992.

[8] Virgil B. Graves, Charles M. Strother, Curtis R. Partington, and Alan Rappe. Flow dynamics of lateral carotid artery aneurysms and their effects on coils and balloons: An experimental study in dogs. *AJNR*, 13:189–196, February 1992.

[9] D. W. Liepsch, H. J. Steiger, A. Poll, and H. J. Reulen. Hemodynamic stress in lateral saccular aneurysms. *Biorheology*, 24:689–710, 1987.

[10] Edward W. Merrill. Rheology of blood. *Physiological Reviews*, 49:863–889, October 1969.

[11] Hideyuki Niimi, Yosuke Kawano, and Ikuo Sugiyama. Structure of blood flow through a curved vessel with an aneurysm. *Biorheology*, 21:603–615, 1984.

[12] Suhas V. Patankar. *Numerical heat transfer and fluid flow.* Hemisphere Publishing Corp., 1980.

[13] H. W. Pia, C. Langmaid, and J. Zierski, editors. *Cerebral Aneurysms.* Springer-Verlag, 1979.

[14] J. N. Reddy. *An Introduction To The Finite Element Method.* McGraw-Hill Book Company, 1984.

[15] John A. Roberson and Clayton T. Crowe. *Engineering Fluid Mechanics.* Houghton Mifflin Company, 3rd edition, 1985.

[16] H. R. Schwarz. *Finite Element Methods.* Academic Press, 1988.

[17] Charles M. Strother, Virgil B. Graves, and Alan Rappe. Aneurysm hemodynamics: An experimental study. *AJNR*, 13:1089–1095, July 1992.

[18] James H. Wood, editor. *Cerebral Blood Flow.* Macgraw Hill, 1987.

Appendix A

Nekton

From [4]:

NEKTON is a computer code for the simulation of steady and unsteady incompressible fluid flow and heat transfer, as well as optional convective-diffusive passive scalar quantities. *NEKTON* is based on the spectral element method, a high-order finite element technique for solution of partial differential equations. The computational domain can be either stationary or moving (free surfaces, moving walls, fluid layers or melting fronts). If both the fluid flow and heat transfer simulation capabilities are used, they can be coupled via forced and/or natural convection heat transfer. A conjugate heat transfer, solid and fluid problem can also be solved.

The package consists of three parts: *PRENEK*, *NEKTON*, and *POSTNEK*.

PRENEK is an interactive menu-driven program in which the user inputs the necessary geometrical parameters (mesh), physical parameters (type of analysis, material properties, boundary conditions, initial conditions), and numerical parameters (discretization, solver, i/o options) to completely specify the computational problem.

NEKTON is the computational module that actually performs the numerical integration of the Navier-Stokes and energy equations.

POSTNEK is an interactive graphical package which allows the user to display and analyze the results of a *NEKTON* simulation.

NEKTON is based on techniques developed by Professor Patera at M.I.T. and Professor Orszag at Princeton.

Appendix B

Aneurysm Blood Flow Visualization

From Flow Visualization of Computational Blood Flow In Artery With Aneurysm, From MS Comprehensive Project by Thanh-Nha T. Do

B.1 Abstract

Flow visualization of blood flow in an intracranial vessel with an aneurysm is implemented first using conventional computer systems and later using virtual reality. A post-processing graphical system using Wavefront's software package, Data Visualizer, is designed to visualize the data produced by the numerical solver. Data Visualizer was developed for scientific visualization with built-in tools for visualization of fluid flow. Velocity profiles and pressure profiles calculated at different times in a systole/diastole cycle are presented as contour plots, cutting planes, iso-surfaces, iso-volumes, arrow plots, streamlines and emitting particles. Animations are done by collecting consecutive outputs from the numerical solver. Discussion of virtual reality as a tool for flow visualization is also presented in this paper.

B.2 Methodologies

Flow visualization using computer graphics is a tool to compare between experimental results and numerical simulation results. Refinement of a model is done by performing iterations between model and observation. Refinement of either the mathematical model or the numerical solution are done based on the discrepancies observed between experimental measurements and results of numerical solution.

Comparison of experimental results and numerical solutions allow validation of the theoretical model. After the computer model is validated, it can replace expensive and time-consuming experiments. Physicians and scientists can use the computer-simulated model to observe the fluid dynamics inside an aneurysm.

B.3 Design and Implementation of Visualization System

Flow visualization for this project is implemented first using conventional computer systems. In a later study, flow visualization will be done using virtual reality. The system of flow visualization is designed based on many standards for flow visualization of computational fluid dynamics. It is designed for physicians as well as scientists.

B.3.1 Flow Visualization Using Conventional Computer Systems

Flow visualization of numerical simulation output can be implemented as three levels: post-processing, tracking and steering Post-processing visualizes pre-calculated results from a numerical solver. Tracking is an interactive process using a real-time display in which the user can terminate a faulty simulation. Steering is an interactive process in which the user is allowed to change parameters as the simulation is running to steer the results of the simulation. In this project, a post-processing graphical system was used to visualize the data produced by the numerical solver.

B.3.1.1 Hardware and Software

Visualization was done on a Silicon Graphics workstation, the iris Power Series 4D, using Data Visualizer. Some software packages developed for flow visualization are Data Visualizer by Wavefront, AVS (Application Visualization System) by Stardent, VP Wave by Precision Visuals, PLOT3D, Surf (Surface Modeler), GAS (Graphical Animations System), FAST (Flow Analysis Software Toolkit), and RIP (Real-time Interface Particle Tracer) by NASA Ames. Data Visualizer developed by Wavefront Technologies, Inc. was most suited to our purposes. Data Visualizer is a software package used for general scientific visualization with special tools for computational fluid dynamics.

B.3.2 Flow Visualization Using Virtual Reality

Virtual reality is also known as virtual worlds, virtual environments, artificial reality, cyberspace and telepresence. Virtual reality is a state-of-the-art technology which combines the knowledge of science, art and technology. It allows the user to become "immersed" in a virtual world created by computers. The relationship between human and machine is tightened. The user can actively communicate with computers instead of passively observing data on the computer screen. Flow visualization using virtual reality permits us to explore the fluid dynamics in an unconventional way. It makes it possible for us to discover new properties and relationships between data. The user can interact with the data in a natural way and the operations of an application are simplified. The user can get familiar with the system quickly and increase the knowledge about the structure of the data and system.

B.3.2.1 Virtual Reality For Visualization of Aneurysms

Virtual reality is a good implementation for this project. Flow visualization of aneurysm is a three-dimensional model which requires three-dimensional controls. The user can view the true object with stereoscopic display and can control directly using natural actions such as grabbing, pointing, pushing and talking.

Visualization of blood flow inside an aneurysm using virtual reality will give the user a special view. The user can place himself inside the aneurysm and observe streamlines as particles are emitted. This will also be a post-processing graphical system. All data would be stored before the mission of virtual reality is carred out. All graphical features of conventional graphic system design are still applied to the virtual reality design. A new user interface must be built. Real-time response is a must in virtual reality. The requirement of virtual systems is that the speed must be at least 10 frames per second.

B.4 Summary

Flow visualization of computational fluid dynamics was done first using conventional systems and will be done later using virtual reality. A post-processing graphical system was implemented to process and display results obtained from a numerical solver. Data Visualizer was recommended

for use as a base for the graphical system and Silicon Graphics workstation was recommended as the platform for the project.

Virtual reality for computational fluid dynamics will make it possible for us to explore data and discover not only the relationships between data as observed by conventional computer systems but also new relationships between data. The interaction between the user and the system is closer. A head-mounted device, a data glove and a graphical workstation are the typical components of a virtual system. Virtual reality has been used in many applications including medical applications.